

PACS numbers: 42.55.Px; 42.60.Da; 42.82.Et
DOI: 10.1070/QE2008v038n03ABEH013725

Numerical study of the influence of thermooptic effects on the competition of modes in diode lasers

D.V. Vysotsky, N.N. Elkin, A.P. Napartovich, V.N. Troshchieva, D. Botez, L.J. Mawst

***Abstract*. A software package is developed for numerical analysis of radiation of edge-emitting diode lasers. The optical block of the package uses the three-dimensional diffraction method of counterpropagating beams. The current carrier density distribution in a quantum well is found from the diffusion equation, and the temperature distribution is found from the heat conduction equation. The software package can be used to analyse the competition of optical modes and to find the critical current at which single-mode lasing is quenched. The operation of a semiconductor laser having a built-in system of waveguides with antiresonance reflection is analysed. The conditions of single-mode generation with the output power above 1 W are found for this laser.**

Keywords: *semiconductor laser, numerical simulation, mode competition, diffraction.*

1. Introduction

Semiconductor lasers emitting a few watts of cw power in a single transverse mode at a wavelength of 980 nm are required for pumping fibre amplifiers and for free space communication. Single-mode oscillation is usually maintained in built-in waveguide single-mode lasers at output powers lower than 1 W [1, 2]. Such lasers employ the asymmetric location of a quantum well to reduce the spatial overlap of the region occupied by the field with the gain region [3, 4], which makes it possible to increase the laser length and output power. At the same time, the width of the emitting spot in the lateral direction (perpendicular to the current direction and optical axis) is restricted by a built-in waveguide and is $\sim 4-5$ μm, so that the maximum output power of the laser is ~ 700 mW in the case of the passivated output surface of the crystal. The increase in the width of the emitting aperture in the lateral direction leads to the excitation of additional modes and degradation of the output beam quality. The main mechanisms producing multimode lasing are the burning of spatial holes and radiation self-focusing due to a change in the refractive index of a medium caused by heating and gradients of the current carrier density. To increase the lateral aperture by preserving single-mode lasing, various arrangements of the elements of the structure are used in recent years, in which the radiation field in the lateral direction is not confined; however, its flow to the side surfaces for a certain mode is small. A waveguide with an antiresonance reflector [5] allowing the efficient selection of the lateral modes by their losses is a successful example of such a structure.

Numerical methods provide reliable calculations of the parameters of semiconductor lasers and amplifiers [6, 7]. In the general case the radiation field in these devices can be calculated by two alternative methods. The method of the field expansion in modes [8] assumes that the modes propagate along the optical axis of a laser (amplifier) without distortions. In this case, the phase incursion is proportional to the laser length with a coefficient called the propagation constant. The mode profile and propagation constant are found by solving the two-dimensional problem on a plane perpendicular to the optical axis by the methods of finite elements [9], lines [10] or finite differences in the time domain (FDTD) [11].

The field can be also calculated by the propagating beam method [12], which allows one to take into account the change in the mode structure during its propagation along the optical axis (the z axis). Such a calculation was performed, for example, in [13] for the case of single-pass amplification at a wavelength of 980 nm. To calculate the lasing regime, it is necessary to take into account the interaction of counterpropagating beams in the active medium [14]. The method of counterpropagating beams often uses the scalar and paraxial approximations, which reduce the problem to the solution of a system of two parabolic equations for the fields of counterpropagating beams. These equations, taking into account the boundary conditions on mirrors and side surfaces, are usually solved by the iteration method [15].

The problem can be often further simplified by using the effective refractive index (ERI) approximation [15, 16], in which the dependences of the field on the transverse (x) and lateral (y) coordinates are separated. In this case, it is sufficient to solve a system of two-dimensional equations in variables x, z. Finally, if the change in the filed amplitude along the optical axis is negligible, the problem is reduced to the solution of a one-dimensional (in the lateral direction) equation [17, 18].

D.V. Vysotsky, N.N. Elkin, A.P. Napartovich, V.N. Troshchieva State Research Center of the Russian Federation, 'Troitsk Institute for Innovation and Fusion Research', 142190 Troitsk, Moscow region, Russia; e-mail: apn@triniti.ru;
D. Botez, L.J. Mawst Reed Center for Photonics, Department of Electrical Computer Engineering, University of Wisconsin-Madison, Madison, WI 53706-1691 USA

Received 23 August 2007
Kvantovaya Elektronika **38** (3) 215–221 (2008)
Translated by M.N. Sapozhnikov

In the case typical for semiconductor lasers, the radiation intensity changes along the z axis by one–two orders of magnitude. The applicability of the ERI approximation depends on the design of an optical waveguide. In particular, it was found that for the ridge structure [19] this approximation was in good agreement with exact calculations. In structures containing piece-parallel waveguides, the separation of the field dependences over coordinates x and y can result in considerable errors [20]. The structure analysed in our paper belongs to this type. It was shown earlier in calculations of the formation of radiation in amplifiers [13] and lasers [21] that the ERI approximation is not valid for structures with built-in waveguides forming antiresonance reflectors.

The analysis of the stability of single-mode oscillation in semiconductor lasers with antiresonance reflectors neglected the influence of the structure heating. The known papers taking the structure heating into account (see, for example, [22, 23]), use the ERI approximation.

In this paper, we describe the three-dimensional model of a diode laser with an antiresonance structure, which generalises the model considered in [21] and takes into account the focusing of radiation caused by the nonuniform heating of the medium. We developed a software package containing the optical unit in which the field of a generated mode is calculated taking into account the inhomogeneous spatial temperature distribution self-consistently with the distribution of current carriers described by the diffusion equation, as in [6]. In addition, the fields of other modes are calculated for the 'frozen' distributions of the gain and refractive index produced by the radiation field of the fundamental mode. The temperature distribution in a sample is found by solving the heat conduction equation, which allows us to study the influence of thermal focusing on the stability of single-mode lasing.

2. Mathematical model

The monochromatic radiation field in a laser in the scalar approximation is described by the Helmholtz equation. In the three-dimensional diffraction calculation of propagating beams [14], the radiation field is represented in the form

$$E(x,y,z) = E_+(x,y,z)\exp(\mathrm{i}k_0 n_0 z) + E_-(x,y,z)\exp(-\mathrm{i}k_0 n_0 z),$$

where k_0 is the wave number of the field in vacuum; n_0 is the mean refractive index; $E_\pm$ are the field amplitudes for counterpropagating beams propagating in the positive (+) and negative (−) directions of the z axis. The propagation of the field along the optical axis is calculated by the method of splitting over diffraction, refraction, and amplification processes. Such a splitting at each of the steps of the numerical calculation makes it possible to describe the inhomogeneities of the gain and refractive index caused by the redistribution of the carrier density and nonuniform heating.

Semiconductor heterostructures have a specific layered structure with layers of width considerably exceeding their thickness [1]. The typical length of the structure along the optical axis is 1–2 mm, the width is 20–40 μm, and the height is 2–4 μm [2]. The amplification occurs in quantum wells of thickness 5–8 nm. The variety of spatial scales requires the use of a fine calculation network with different steps along different axes. We used the orthogonal network of size 256×256 in the cross section with the cell size along the optical axis equal to 0.1 μm, which requires $10^4 - 2\times 10^4$ steps along the z axis for the typical length of a crystal 1–2 mm.

The absence of reflection of radiation incident on the boundaries of the calculation region is provided by the perfectly matched layer boundary condition [24] in the variant [25] developed for waveguide structures.

Because the typical dimensions of structures in a semiconductor laser in a plane perpendicular to its optical axis are comparable with the radiation wavelength, the diffraction of radiation is described in the wide-angle Pade approximation [26]. We use one of the variants of this approximation in which the beam field amplitudes are described by the equations [27]

$$\pm\left(1 - \frac{\mathrm{i}b}{4k_0 n_0} + \frac{1}{4k_0^2 n_0^2}\Delta_\perp\right)\frac{\partial E_\pm}{\partial z} - \frac{\mathrm{i}}{2k_0 n_0}\Delta_\perp E_\pm - \frac{b}{2}E_\pm = 0, \quad (1)$$

where

$$\Delta_\perp = \frac{\partial^2}{\partial x^2} + \frac{\partial^2}{\partial y^2}; \quad b = g - \alpha + \frac{\mathrm{i}k_0}{n_0}\left(n^2 - n_0^2\right);$$

n is the local refractive index; α is the coefficient of distributed optical losses; and g is the gain, which is negative if the injection current density is lower than current density at which the medium becomes transparent (transparency current density).

In the general case the relation between the gain and concentration of carriers in a quantum well has a complicated form and should be found by solving the continuity equation for the electron and hole flows [28]. The acceptable accuracy for structures being simulated is provided by the logarithmic approximation [13]. The current carrier density N in quantum wells was determined by solving the one-dimensional lateral-direction diffusion equation [29]

$$\frac{\partial^2 Y}{\partial y^2} - \frac{Y}{D\tau_{\mathrm{nr}}} - \frac{B}{D}N_{\mathrm{tr}}Y^2 - \frac{g}{g_{0N}D\tau_{\mathrm{nr}}}|U|^2 = -\frac{J}{qDd_{\mathrm{w}}N_{\mathrm{tr}}}, \quad (2)$$

where $Y = N/N_{\mathrm{tr}}$; D is the carrier diffusion coefficient; τ_{nr} is the linear recombination time; $g_{0N} = g(Y = \mathrm{e})$; B is the coefficient characterising the carrier loss quadratic in concentration; $|U|^2 = |E_+ + E_-|^2/I_{\mathrm{s}}$; $I_{\mathrm{s}} = hcN_{\mathrm{tr}}/(\lambda g_{0N}\tau_{\mathrm{nr}})$ is the saturation intensity; h is Planck's constant; λ is the wavelength; c is the speed of light; J is the pump current density; $N_{\mathrm{tr}} = \{-\tau_{\mathrm{nr}}^{-1} + [\tau_{\mathrm{nr}}^{-2} + 4BJ_{\mathrm{tr}}(qd_{\mathrm{w}})]^{1/2}\}/(2B)$ is the current carrier density corresponding to the zero amplification and absorption; J_{tr} is the transparency current density; q is the electron charge; and d_{w} is the quantum well thickness. The Auger recombination loss, proportional to the third power of the carrier concentration, is neglected in this calculation. The refractive index in a quantum well is defined as $\tilde{n} = \tilde{n}_0 - Rg/(2k_0) + vT$, where n_0 is the refractive index corresponding to the transparency current; R is the line enhancement factor; v is the thermooptic coefficient; and T is the change in the quantum-well temperature with

Table 1.

J_{tr}/A cm^{-2}	g_{0N}/cm^{-1}	α/cm^{-1}	B/cm^3 s^{-1}	R	τ_{nr}/ns	D/cm^2 s^{-1}	d_w/nm	λ/μm	r_1	r_2	v/K^{-1}
50	2200	1.5	10^{-10}	2	1	100	8.5	0.98	0.95	0.01	3×10^{-4}

Note: $r_{1,2}$ are reflectances of the resonator mirrors.

respect to the temperature of a cooler. All these parameters depend on materials and the heterostructure type. The values of parameters used in calculations are presented in Table 1. The thermooptic coefficient was assumed the same for all layers.

The temperature distribution in a sample was found by solving the two-dimensional heat conduction equation

$$-\frac{\partial}{\partial x}\left(\chi\frac{\partial T}{\partial x}\right)-\frac{\partial}{\partial y}\left(\chi\frac{\partial T}{\partial y}\right)=f \qquad (3)$$

in a plane perpendicular to the optical axis. Here, χ is the heat conductivity and the heat source function f includes the ohmic loss ρJ^2 (ρ is the ohmic resistance) and heating related to the thermalisation of electrons and holes in the quantum well. Our main goal was to find temperature gradients in the irradiated region rather than the absolute value of the temperature. We neglected the nonlinear recombination of carriers and spontaneous radiation in the thermal balance because the contribution of these processes for a 980-nm laser analysed in the paper is insignificant. The distributed laser radiation loss is usually caused by radiation scattering from structural defects and its contribution to the thermal balance is also insignificant. In the case of such simplifications, the temperature along the optical axis does not change. The region of calculations for solving the heat conduction equation considerably exceeds the region of calculations for optical modes. The temperature is assumed specified at the boundary with a cooler, so that the temperature increment is zero, while at the other boundaries the heat flow $\partial T/\partial \boldsymbol{n}$ was assumed zero (where $\boldsymbol{n}$ is the normal to the boundary).

The found distributions of the temperature increment were used to recalculate the local refractive index by the expression

$$n(T)=n|_{T=0}+vT. \qquad (4)$$

The radiation field distribution matched with the temperature and carrier concentration distributions in the quantum well for the specified pump current profile was calculated by the Fox–Li method.

For the specified gain and refractive index distributions, produced by the generated mode, we calculated the field distributions for other modes, for which the gain was lower than the threshold, and calculated lasing thresholds for each of them [30]. A similar approach was used in paper [15] to calculate the discrimination of modes in a laser without a built-in waveguide by employing the ERI approximation and neglecting heating. By calculating the lasing thresholds for higher-order modes, we can find injection currents at which the gains for competing modes achieve threshold values. In this way, the maximum single-mode output power is determined for the given sample. The determination of a set of competing modes is reduced to a linear eigenvalue problem for Eqn (1) with the specified functions n and g. This problem was solved by the shift and invert Arnoldi method [31]. The use of this method to simulate a diode laser is described in detail in paper [27].

3. Calculation results and discussion

3.1 Calculation of the fundamental-mode generation

Figure 1a shows the simplified scheme of the section of a sample perpendicular to the optical axis (without following the spatial scale). Heat is removed through a number of layers: a 100-nm-thick titanium contact; two 5-μm-thick gold layers separated by a 5-μm-thick AuSn solder layer; and a 200-μm-thick CuW layer. The thickness of a GaAs substrate was 124 μm, so that the size of the total region for calculating the heat conduction was 342 × 500 μm. Figure 1b shows schematically the region in which laser radiation is concentrated. The material and thickness of layers in this region are presented in Table 2 in paper [13]. The sample represents in the section a heterostructure with a separate confinement and the small optical mode confinement factor Γ ($\Gamma = 1.1\,\%$ in the central element).

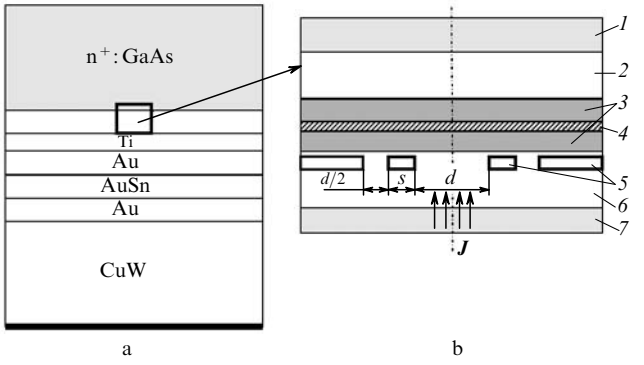

Figure 1. Cross section of a laser with a system of coupled antiresonance waveguides. The region of calculation of the heat conduction equation (below is shown the boundary of a cooler at fixed temperature) (a) and the cross section of the region of calculation of optical modes (b): (*1*) substrate; (*2*) n-plate; (*3*) optical waveguide; (*4*) active layer (quantum well); (*5*) built-in waveguides; (*6*) p-plate; (*7*) p-GaAs layer.

The laser design has a property that for a mode whose field in the lateral direction can be represented in the form of a half-wave in the central element of width d, the side elements of width $d/2$ play the role of a quarter-wave plate well reflecting the incident radiation [5]. For higher-order modes, the interference of the fields outside the central element leads to the intense radiation flow outside. Thus, this structure is the antiwaveguide one (the effective refractive index in the central element is lower than that in region of waveguide inserts), and radiation losses in the lateral direction for all modes are large compared to the fundamental-mode loss. By varying the width s of waveguide inserts, it is possible to change the lateral radiation loss in a broad range. The aim of our study is to find the

value of s at which the maximum single-mode radiation power is achieved.

As the pump current is increased, the amplification is saturated and becomes more inhomogeneous. In this case, higher-order modes are amplified stronger and single-mode lasing is quenched. The numerical simulation of the laser with the optical structure shown in Fig. 1b was performed in paper [17] in the ERI approximation and in paper [21] by the method of counterpropagating beams by neglecting heating. It was found in [21] that the abandonment of the ERI approximation resulted in considerable changes in the critical parameters found for single-mode lasing. In particular, the limiting power for samples with inserts of width s providing the minimal lateral radiation loss for the fundamental mode proved to be lower than that for other s. The insert widths were determined at which the single-mode output power could exceed ~ 1 W. However, estimates show that heating cannot be neglected at such powers. We will present below the results of numerical simulation of this structure taking into account thermal focusing.

For comparison with previous papers [17, 21], we studied a sample of length 2 mm with the central element of width $d = 10$ μm and the reflectances of the output and highly reflecting mirrors equal to 1 % and 95 %, respectively. The model also includes the distributed radiation loss with the coefficient $\alpha = 1.5$ cm^{-1}. The calculation of radiation generation in such a laser for the specified pumping takes 15 – 30 hours by using a 2.4-GHz Pentium IV PC. It was shown earlier [21] that calculations of generation in a laser with a shorter crystal and mirror reflectances providing the preservation of the threshold gain did not change parametric dependences. Therefore, for calculations with the variable width s, the laser length was reduced by an order of magnitude (down to 0.2 mm). In this case, the reflectances of the resonator mirrors were 63.1 % and 99.5 %.

The pump current density was assumed constant within the central element and zero outside it. This approximation is reasonable in this case because the 'flowing out' of the current outside the central element can be limited by blocking layers on both sides of the antiwaveguide [32].

Figure 2 shows the light – current characteristic calculated for a laser of length 0.2 mm with waveguide inserts of width 2.6 μm. For comparison, the light – current characteristic calculated by neglecting heating is also shown. One can see that the slope of this characteristic increases due to nonuniform heating. This is explained by the fact that nonuniform heating causes the focusing of the fundamental-mode field to the central element region, thereby reducing the lateral radiation loss. Figure 3 shows the calculated distribution of the normalised temperature increment in the quantum well over the lateral coordinate. This profile weakly depends on the width of waveguide inserts. The maximum temperature increment as a function of the pump current related to the transparency current is shown in Fig. 4.

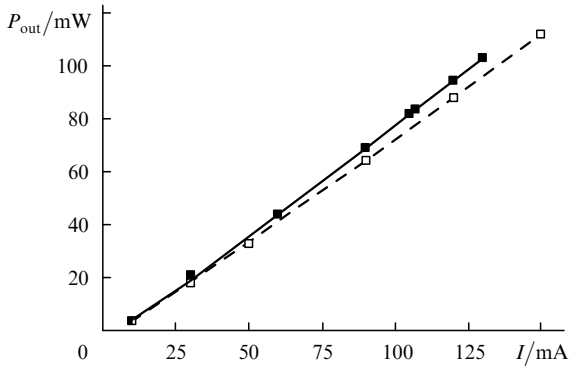

Figure 2. Dependences of the output radiation power P_{out} on the pump current I calculated for waveguide inserts of width $s = 2.6$ μm and the laser length 0.2 mm taking thermal focusing into account (■) and neglecting it (□).

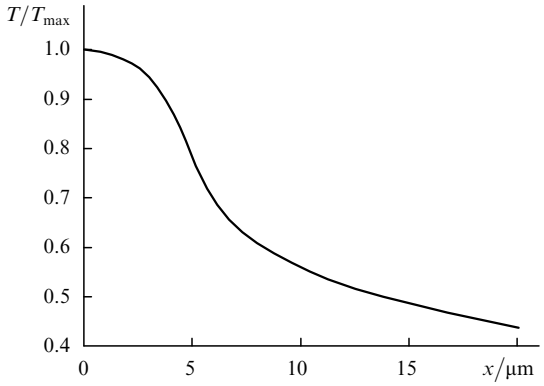

Figure 3. Temperature increment with respect to the environment temperature normalised to the maximum value T_{max} calculated for waveguide inserts of width $s = 2.6$ μm and the laser length 0.2 mm.

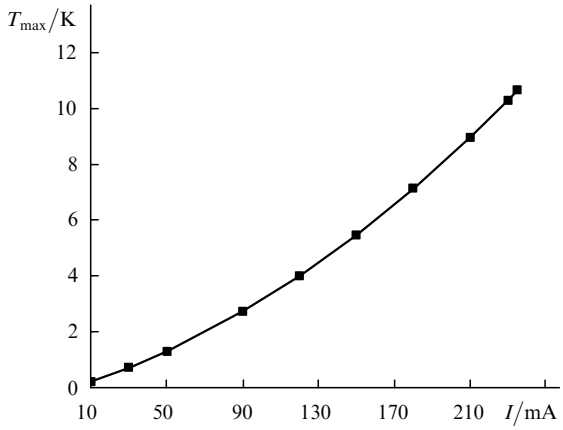

Figure 4. Maximum change of the temperature T_{max} in a laser compared to the environment temperature as a function of the pump current I calculated for waveguide inserts of width $s = 2.6$ μm and the laser length 0.2 mm.

The generation in the laser of length 0.2 mm was calculated for different widths s of waveguide inserts. It was found in [21] that for rather low pump currents, when the estimated heating is insignificant (such a situation is realised in the case of pulsed lasing), single-mode lasing is quenched for $s = 2 - 2.4$ μm. Our calculations confirmed that the role of heating for such values of s is insignificant and the achievable single-mode lasing power is small ($\sim 15 - 20$ mW).

Figure 5 presents light – current characteristics calculated for the values of s at which single-mode lasing remains stable at pump powers exceeding the lasing threshold by 40 – 50 times. Unlike the predictions of the optical

model [21], the theory taking into account the sample heating predicts the presence of a break in the light–current characteristics ($s = 1.6$, 2.7, and 2.8 μm) at the pump current densities exceeding the transparency current density approximately by two orders of magnitude (the pump current density exceeds the threshold value approximately by a factor of 20). This break appears due to thermal focusing, which increases the fraction of the radiation power contained in the central element, thereby enhancing the lasing efficiency. The calculated lasing thresholds proved to be highest for these values of s, which suggests that the lateral radiation loss is high at low pump currents. Such a laser design is usually not used in experiments because it is assumed that the lasing efficiency will be low. Our model predicts that it is in this case that the stability of the single-mode regime is maximal, and the lasing efficiency increases with the pump current.

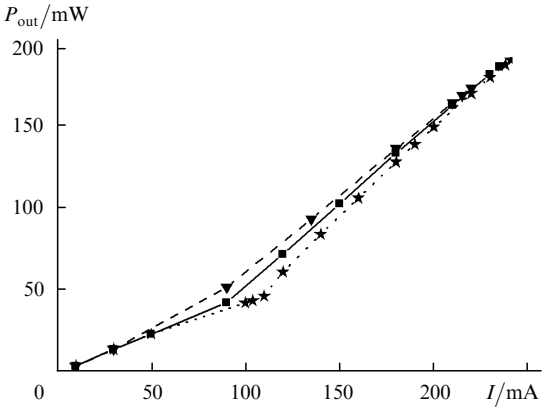

Figure 5. Dependence of the output power P_{out} on the pump current I for a laser of length 0.2 mm with waveguide inserts of width $s = 1.6$ (★), 2.7 (▼), and 2.8 μm (■).

3.2 Calculation of competing modes and the maximum single-model lasing power

After calculating the fundamental mode for the given s and fixed pumped current, we calculated higher-order modes, which can compete with the generated mode. These calculations gave the spatial structures of modes and their eigenvalues γ. The moduli of eigenvalues determine the closeness of the gains of corresponding modes to the lasing threshold. As the pump current is increased, the moduli of eigenvalues of some modes increase, and when one of the moduli achieves unity, lasing appears at the corresponding mode. The pump current at this moment is the critical current at which single-mode lasing becomes unstable.

Figure 6 presents the dependences of the modulus of the eigenvalue of the mode nearest to the lasing threshold on the ratio of the pump current density to the transparency current density for $s = 2.6$ μm calculated by taking thermal focusing into account and neglecting it. The calculations were performed for the short (0.2 mm) and long (2 mm) samples. One can see from Fig. 6 that the dependence of eigenvalues on the pump current drastically changes upon heating. A break appears in the curves, which indicates that the competing mode changes with increasing pump current. The critical pump current density is higher for the long

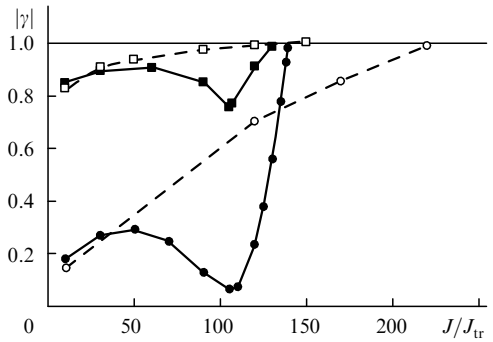

Figure 6. Moduli $|\gamma|$ of the eigenvalue of the mode nearest to the lasing threshold as a function of the pump current density J normalised to the transparency current density J_{tr}. Calculations are performed taking thermal self-focusing into account (solid curves) and neglecting it (dashed curves) for $s = 2.6$ μm and the laser length 0.2 (squares) and 2 mm (circles).

sample than for the short one in both models; however, these current densities considerably approach each other upon heating for both models.

To elucidate the mechanisms leading to the effects observed, we consider changes in the field profiles of two modes with the highest eigenvalues with increasing pump current for the short sample with $s = 2.6$ μm. Figure 7 shows the structure of these modes in the near-field region for three pump currents $I = 10$, 107, and 130 mA. If the mode is characterised by the number of changes in the field sign, then upon weak pumping mode 7, whose field is concentrated in the central element, is closer to the threshold. The field of this mode in the central element is defocused and redistributed into side elements due to the thermally induced increase in the refractive index. Defocusing enhances the lateral radiation loss and reduces $|\gamma|$ for $I > 50$ mA. Competing mode 5, on the contrary, is focused to the centre, which is accompanied by a decrease in the lateral radiation loss and a better spatial overlap of the region occupied by the field with the region in which amplification occurs. As a result, for the current $I =$ 100 mA, the excess over the threshold for mode 5 becomes equal to that for mode 7, and for $I \sim 130$ mA, lasing appears at mode 5.

Figure 8 illustrates the fact that, as the sample length is increased by a factor of 10 (up to 2 mm), the slope of the light–current characteristic changes weakly both in the optical and thermal models. At the same time, irrespective of the sample length, the slope of the light–current characteristic is larger in the model taking heating into account. The influence of heating on the competition of modes for the long sample with $s = 2.6$ μm strongly reduces the maximum single-mode laser power from 1.42 to 1 W.

4. Conclusions

We have analysed numerically the stability of single-mode oscillation in a semiconductor laser with a system of built-in waveguides with antiresonance reflection. The software package has been briefly described which includes the three-dimensional optical block based on the method of counter-propagating beams and the thermal block for calculating the temperature profile. The package provides the self-consistent solution of the diffraction optic equation, the diffusion equation for current carriers in a quantum well

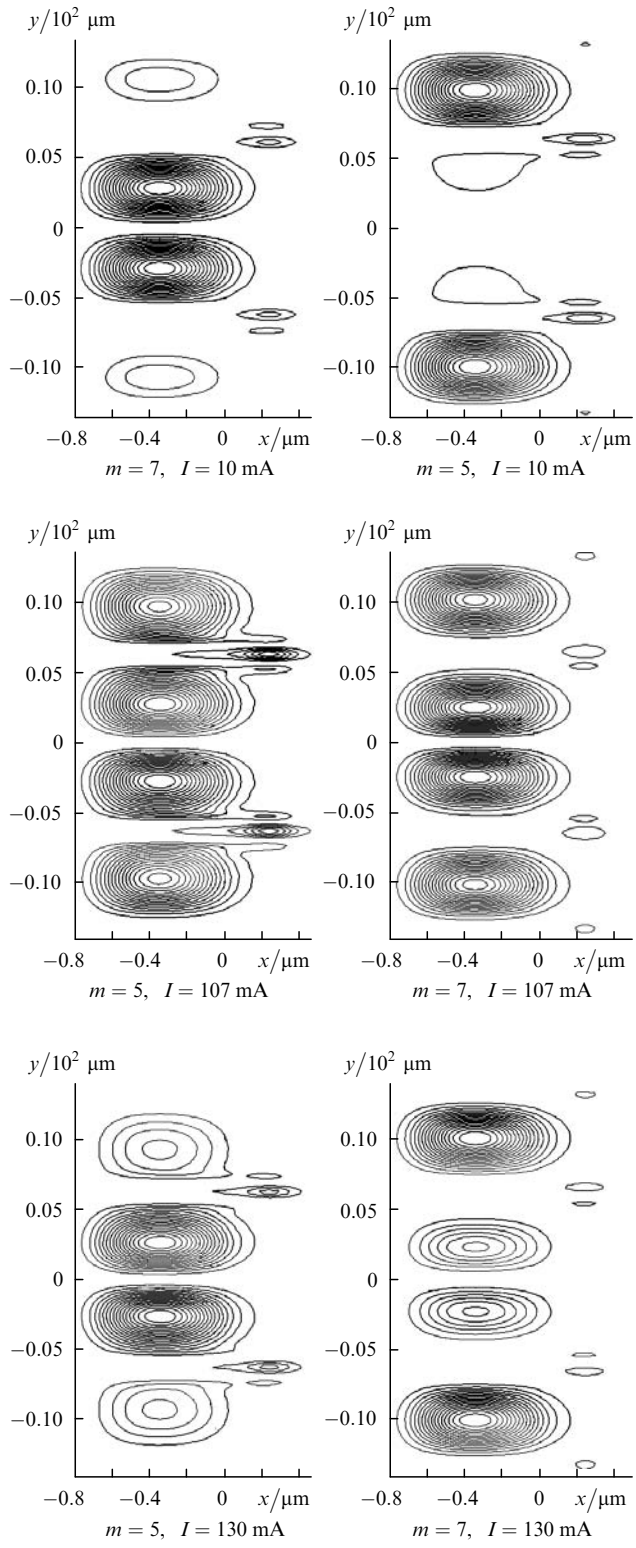

Figure 7. Near-field radiation intensity distributions for modes with numbers $m = 5$ and 7 competing with the generated mode (left and right columns show the modes nearest and next-to-nearest to the lasing threshold, respectively) at different pump currents, the width of waveguide inserts $s = 2.6$ μm and the laser length 0.2 mm.

and the heat conduction equation. The gains and losses have been calculated for competing modes taking into account the refractive-index and gain distributions produced by the generated mode. This allows us to predict the stability limit of single-mode lasing over current.

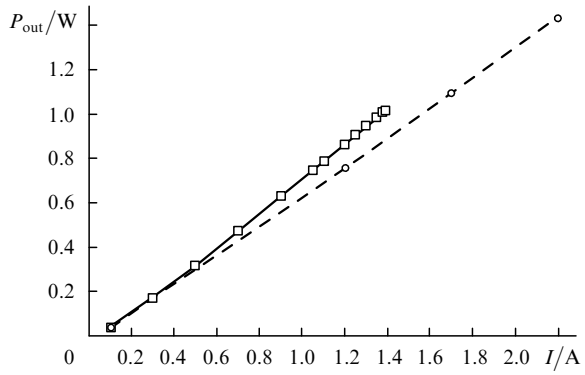

Figure 8. Dependences of the output power P_{out} of the laser of length 2 mm on the pump current I for the width of waveguide inserts $s = 2.6$ μm calculated by taking thermal focusing into account (□) and neglecting it (○).

It has been predicted in [21] that maximum single-mode powers are achieved near the lateral radiation transmission resonance. However, the maximum power could not be calculated reliably within the framework of the optical model because estimates showed the important role of a thermal lens induced by sample heating. We have found in this paper that thermal focusing enhances the slope efficiency of the laser. In a laser with a waveguide insert of width corresponding to the maximum lateral radiation loss at a low current, the slope efficiency increases with the pump current. The maximum single-mode power for a laser of length 2 mm with $s = 2.6$ μm is predicted to be ~ 1 W.

Acknowledgements. The authors from SRC RF TRINITI thank A.P. Bogatov for useful discussions. This work was supported by the Russian Foundation for Basic Research (Grant No.05-02-16769-a).

References

1. Gokhale M.R., Dries J.C., Studenkov P.V., Forrest S.R., Garbuzov D.Z. *IEEE J. Quantum Electron.*, **33**, 2266 (1997).
2. Slipchenko S.O., Pikhtin N.A., Fetisova N.V., Khomylev M.A., Marmalyuk A.A., Nikitin D.B., Padalitsa A.A., Bulaev P.V., Zalevskii I.D., Tarasov I.S. *Pis'ma Zh. Tekh. Fiz.*, **29**, 65 (2003).
3. Al-Muhanna A., Mawst L.J., Botez D., Garbuzov D.Z., Martinelli R.U., Connoly J.C. *Appl. Phys. Lett.*, **73**, 1182 (1998).
4. Donelli J.P., Huang R.K., Walpole J.N., Missaggia L.J., Harris C.T., Plant J.J., Bailey R.J., Mull D.E., Goodhue W.D., Turner G.V. *IEEE J. Quantum Electron.*, **39**, 289 (2003).
5. Mawst L.J., Botez D., Zmudzinski C., Tu C. *Appl. Phys. Lett.*, **61**, 503 (1992).
6. Hadley G.R., in *Diode Laser Arrays*. Ed. by D. Botez, D.R. Scifres (Cambridge, UK: Cambridge Univ. Press, 1994) pp 180 – 225.
7. Scarmozzino R., Gopinath A., Pregla R., Helfert S. *IEEE J. Sel. Top. Quantum Electron.*, **6**, 150 (2000).
8. Witzigmann B., Witzig A., Fichtner W. *IEEE Trans. Electr. Dev.*, **47** (10), 1926 (2000).
9. Tsuji Y., Koshiba M. *IEEE J. Sel. Top. Quantum Electron.*, **6**, 163 (2000).
10. Rogge U., Pregla R. *J. Lightwave Technol.*, **11**, 2015 (1993).
11. Hayes P., O'Keefe M., Woodward P., Gopinath A. *Opt. Quantum Electron.*, **31**, 813 (1999).
12. Feit M.D., Fleck J.A. *Appl. Opt.*, **17**, 3990 (1978).
13. Vysotsky D.V., Elkin N.N., Napartovich A.P., Sukharev A.G., Troshchieva V.N. *Kvantovaya Elektron.*, **36**, 309 (2006) [*Quantum Electron.*, **36**, 309 (2006)].

14. Rao H., Scarmozzino R., Osgood R.M. Jr. *IEEE Photon. Techn. Lett*., **11**, 830 (1999).
15. Lim J.J., Benson T.M., Larkins E.C. *IEEE J. Quantum Electron*., **41**, 506 (2005).
16. Buus J. *IEEE J. Quantum Electron*., **18**, 1083 (1982).
17. Chang J.C., Lee J.J., Al-Muhanna A., Mawst L.J., Botez D. *Appl. Phys. Lett*., **81**, 1 (2002).
18. Mawst L.J., Botez D., Zmudzinski C., Tu C. *IEEE Photon. Techn. Lett*., **4**, 1204 (1992).
19. Batrak D.V., Plisyuk S.A. *Kvantovaya Elektron*., **36**, 349 (2006) [*Quantum Electron*., **36**, 349 (2006)].
20. Botez D., in *Diode Laser Arrays*. Ed. by D. Botez, D.R. Scifres (Cambridge, UK: Cambridge Univ. Press, 1994) pp 1 – 71.
21. Napartovich A.P., Elkin N.N., Sukharev A.G., Troshchieva V.N., Vysotsky D.V., Nesnidal M., Stiers E., Mawst L.J., Botez D. *IEEE J. Quantum Electron*., **42**, 589 (2006).
22. Dai Z., Michalzik R., Unger P., Ebeling K.J. *IEEE J. Quantum Electron*., **33**, 2240 (1997).
23. Plisyuk S.A., Batrak D.V., Drakin A.E., Bogatov A.P. *Kvantovaya Elektron*., **36**, 989 (2006) [*Quantum Electron*., **36**, 989 (2006)].
24. Berenger J.P. *J. Comput. Phys*., **114**, 185 (1994).
25. Huang W.P., Xu C.G., Lui W., Yokoyama K. *IEEE Phot. Techn. Lett*., **8**, 652 (1996).
26. Hadley G.R. *Opt. Lett*., **17**, 1426 (1992).
27. Elkin N.N., Napartovich A.P., Sukharev A.G., Vysotsky D.V. *Lect. Notes Comp. Sci*., **3401**, 272 (2005).
28. Coldren L.A., Corzine S.W. *Diode Lasers and Photonic Integrated Circuits* (New York: Wiley, 1995).
29. Hadley G.R., Hohimer J.P., Owyoung A. *IEEE J. Quantum Electron*., **23**, 765 (1987).
30. Elkin N.N., Napartovich A.P. *Prikladnaya optika lazerov* (Applied Laser Optics) (Moscow: TsNIIatominform, 1989).
31. Demmel J.M. *Applied Numerical Linear Algebra* (Philadelphia, PA, SIAM, 1997).
32. Yang H., Nesnidal M., Al-Muhanna A., Mawst L.J., Botez D., Vang T.A., Alvarez F.D., Johnson R. *IEEE Photon. Techn. Lett*., **10** (8), 1079 (1998).